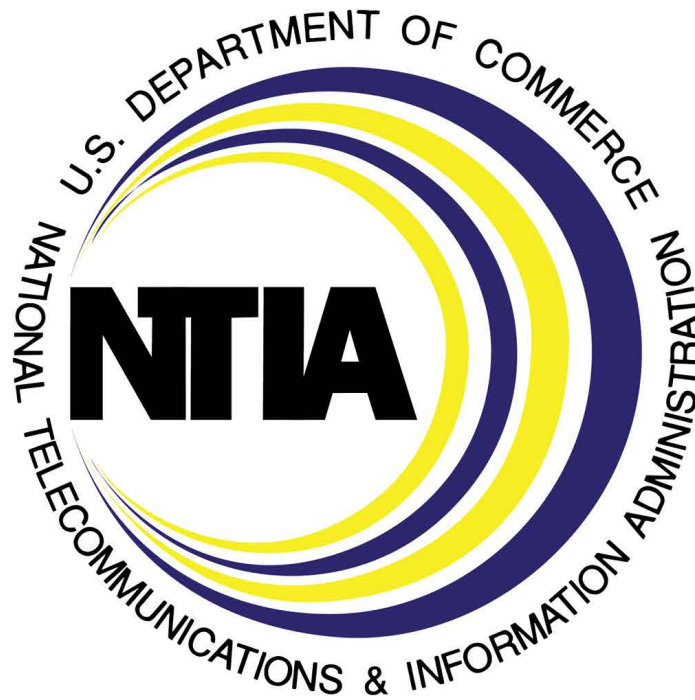


Tropospheric Scatter: Theory vs. Predictive Models

Roger Dalke



Technical Report

Tropospheric Scatter: Theory vs. Predictive Models

Roger Dalke



U.S. DEPARTMENT OF COMMERCE

Alan Davidson
Assistant Secretary of Commerce for Communications and Information
National Telecommunications and Information Administration

February 2022

CONTENTS

Figures	iv
1 Introduction	1
2 Electromagnetic Theory	3
3 Evaluation of the Common Volume Integral	8
3.1 Analytic Solutions	9
3.2 Numerical Solutions	10
3.3 The Numerical Integration Algorithm	12
3.4 A Formal Result	12
4 Theory vs. Propagation Models	15
4.1 Theory vs. Models When Frequency Gain Is Negligible	15
4.2 Frequency Gain for a Constant Refractive Index $\eta = 0$ and $\rho_{1,2} < \infty$	17
4.3 Theory vs. Models When Frequency Gain Is Not Negligible	18
5 Conclusions	24
6 References	25
Appendix A: The Many Integrals of V^2	26
Appendix B: Constant Refractivity Frequency Gain	29

FIGURES

Figure 1.	Geometry for the scatter integral	8
Figure 2.	$\eta_s = 1$, asymmetry factor=1, $\rho_2 = 1$	19
Figure 3.	$\eta_s = 3$, asymmetry factor=1, $\rho_2 = 1$	20
Figure 4.	$\eta_s = 5$, asymmetry factor=1, $\rho_2 = 1$	20
Figure 5.	$\eta_s = 1$, asymmetry factor=1/4, $\rho_2 = 1$	21
Figure 6.	$\eta_s = 3$, asymmetry factor=1/4, $\rho_2 = 1$	21
Figure 7.	$\eta_s = 5$, asymmetry factor=1/4, $\rho_2 = 1$	22
Figure 8.	$\eta_s = 1$, asymmetry factor=1/10, $\rho_2 = 1$	22
Figure 9.	$\eta_s = 3$, asymmetry factor=1/10, $\rho_2 = 1$	23
Figure 10.	$\eta_s = 5$, asymmetry factor=1/10, $\rho_2 = 1$	23

TROPOSPHERIC SCATTER: THEORY VS. PREDICTIVE MODELS

Roger Dalke¹

Circa 1960, the National Bureau of Standards intensively studied over-the-horizon radio propagation due to tropospheric (aka forward) scatter. The results of that effort, published in the form of graphs and/or empirical mathematical functions based on curve fitting, led to the development of important radio propagation models. Unfortunately, there is scant documentation describing exactly how the published data is related to the underlying theoretical basis for scattering theory. In this report, we describe the electromagnetic theory that results in the forward scatter Common Volume Integral. This is followed by a description of analytical methods used to obtain solutions. The results are then compared to propagation model predictions. In general, fairly good agreement between theory and models was obtained for the Irregular Terrain Model and IF-73 air/ground propagation model. Good agreement with the IF-77 Electromagnetic Wave Propagation Model was obtained when frequency gain corrections are negligible. Otherwise, the IF-77 and theoretical results differed significantly. The reason for this was not determined.

Keywords: tropospheric scatter, forward scatter, Irregular Terrain Model, IF-77 Electromagnetic Wave Propagation Model

1 INTRODUCTION

It is well known that over the horizon microwave signals can be received at large distances due to irregularities in the atmospheric index of refraction [1]. This phenomenon is called tropospheric or forward scatter and was the subject of intense study by researchers at the National Bureau of Standard's Central Radio Propagation Laboratory ("the NBS group" [1]). The results of their efforts, described in NBS Technical Notes 15 and 101 [2, 3], led to the development of important radio propagation models [4, 5] that are commonly used to predict radio signal attenuation.

There are numerous publications describing early efforts to understand forward scatter (see e.g., [6, 7, 8]). In particular, [7, 8] provide a detailed description of methods used to calculate forward scatter attenuation based on Booker-Gordon turbulence theory [9] along with the assumption that *scattering efficiency* varies in proportion to the *inverse height* above the earth's surface. Further research resulted in a quite different formulation as noted by [1, p. 225]:

The NBS group has used the meteorologically observed *exponential variation* [emphasis added] of $d\epsilon_0/dh$ up to stratospheric heights to predict experimental data [e.g., attenuation] presented in figure 22 quite well out to 700 miles ...

¹The author is with the Institute for Telecommunication Sciences, National Telecommunications and Information Administration, U.S. Department of Commerce, Boulder, Colorado 80305.

The problem has only been solved completely by the NBS group, using numerical techniques ... They considered broad-antenna patterns with the mixing-in-gradient model and obtained good (absolute) agreement with experimental data.

NBS Technical Note 15 and an “unpublished work” are cited as a source for these comments. We see then that NBS Technical Notes 15 and 101 and hence the propagation models [4, 5] are not wholly based on the theory presented in [6, 7, 8].

The NBS Technical Notes provide detailed methods for predicting forward scatter attenuation in the form of data and equations involving elementary functions; evidently, the equations are based on curve fitting. There is scant information on how these data are related to fundamental tropospheric scatter theory. In fact, in the forward to NBS Technical Note 15 [2], we find the following statement:

Within a year it is hoped to submit for publication in the NBS Journal of Research, Part D, a detailed explanation of the prediction methods of this Technical Note, greatly simplified without loss of accuracy, and including a discussion of the theory.

We have been unable to locate such a document. Furthermore, the forward to NBS Technical Note 101 [3], published several years after Technical Note 15, states

further development of forward scatter predictions and a better understanding of the refractive index structure of the atmosphere led to changes reported in an early *unpublished* [emphasis added] NBS report and in NBS Technical Note 15.

Then in [5] we find a section titled “Scatter Region” followed by four pages of cryptic equations that are used to calculate attenuation due to tropospheric scatter. The only reference is to an *informal communication* by Dr. George Hufford. This dearth of formal publications that describe exactly the theoretical basis for the models is, unfortunately, what we often found in our quest to understand the basis for the data and equations presented in [2, 3, 5].

Recently, there have been questions regarding the efficacy of these models when it comes to forward scatter predictions. Evidently, the published record does not adequately describe the relationship between propagation model predictions and electromagnetic theory. To bridge this knowledge gap, the main purpose of this effort is to compare theoretical results and model predictions. To accomplish this task, the “somewhat difficult” forward scatter integrals were evaluated.

First, we describe in some detail the electromagnetic theory of forward scatter that culminates in the so called *Common Volume Integral*. That is purportedly the basis for propagation model forward scattering algorithms. Next, methods used to evaluate the integral are described in some detail. Finally, calculated theoretical results are compared with those obtained via various propagation model algorithms.

2 ELECTROMAGNETIC THEORY

The mathematical details contained in this section are based on unpublished notes created by Dr. George Hufford, where he states: “the description that follows is a standard one used in such publications as Tech Note 101.”

We assume that the transmitter is at the point x_1 and the receiver is *over the horizon* at point x_2 (see Figure 1). The transmitted radio field $u(x)$ satisfies the Helmholtz equation

$$\nabla^2 u + k^2(1 + 2N)u = \delta(x - x_1) \quad (1)$$

where k is the propagation constant and the refractivity, $N = N(x)$, is a stochastic function of space with mean $\bar{N} = \mathcal{E}\{N\}$. The refractivity may also be a function of time and it is assumed that its mean is a smooth function of space and independent of time.

Suppose that $u = U + \hat{u}$ where U depends on \bar{N} and \hat{u} represents a perturbation that depends on the stochastic refractivity deviation $\varepsilon = N - \bar{N}$. We then have

$$\nabla^2 U + k^2(1 + 2\bar{N})U - \delta(x - x_1) + \nabla^2 \hat{u} + k^2(1 + 2\bar{N})\hat{u} + 2k^2\varepsilon u = 0. \quad (2)$$

Let $U(x, x_1)$ be a *Green's* function that depends on the mean refractivity and also satisfies the (homogeneous) boundary condition imposed by the obstructive earth; we then have

$$\nabla^2 U + k^2(1 + 2\bar{N})U = \delta(x - x_1) \quad (3)$$

$$\nabla^2 \hat{u} + k^2(1 + 2\bar{N})\hat{u} = -2k^2\varepsilon u \quad (4)$$

where

$$\hat{u}(x) = -2k^2 \int U(x, x')\varepsilon(x')u(x')dx'. \quad (5)$$

Note that U can be large only if the points x and x_1 are within sight of each other. An integral equation for the radio field $u(x)$ is easily obtained, viz.

$$u(x) = U(x, x_1) - 2k^2 \int U(x, x')\varepsilon(x')u(x')dx'. \quad (6)$$

Since $u(x) = U(x, x_1) + \hat{u}(x)$ and \hat{u} represents ostensibly small deviations, the iteration-perturbation method may be used to find an approximate solution to the integral equation. This involves substituting the unperturbed function $U(x, x_1)$ for $u(x)$ under the integral sign, then this process is repeated using that solution and so on. Only the first iteration is used; this is known as the Born single scattering approximation. The radio field at the receiver is then

$$\begin{aligned} u(x_2) &\approx U(x_2, x_1) - 2k^2 \int U(x_2, x)U(x, x_1)\varepsilon(x)dx \\ &= u_d + u_s \end{aligned} \quad (7)$$

where u_d is the diffraction field and u_s is the forward scatter field.

The integral represents the sum of many elemental signals scattered by random refractivity deviations. The deviations are zero-mean and considering the central limit theorem, u_s is a zero-mean Gaussian random process. Thus, the average received power $\mathcal{E}\{|u_s|^2\}$ is required to describe the process. Also, with the addition of the diffracted field, a constant, the radio field distribution is Nakagami-Rice.

Propagation models usually calculate the gain (or attenuation) relative to the free-space field based on the great circle distance ℓ between terminals. For a point source, the free-space field is $u_{fs} = -e^{ik\ell}/4\pi\ell$, hence, the function of interest is v_s , where

$$u_s = -\frac{e^{ik\ell}}{4\pi\ell}v_s. \quad (8)$$

Based on the radio frequencies of interest and typical distances from the points x_1 and x_2 to the *commonly viewed* scattering elements, ray theory is used to describe U within the scattering integral, viz.,

$$U(x, x_i) = -g_i(x) \frac{e^{ik\psi_i(x)}}{4\pi r_i} \quad (9)$$

where $r_i = |x - x_i|$ and $\psi_i(x)$ is the *optical length* of the rays coming from the transmitter and going to the receiver. Note that the integral is over the commonly viewed elements, so that region is called the *common volume* \mathcal{V} .

The function $g_i(x)$ represents the *field* gain from the antenna at x_i (in principle it should include the relatively small diffracted field). The scattered field relative to free space is then

$$v_s = \frac{k^2\ell}{2\pi} \int g_1(x)g_2(x) \frac{1}{r_1r_2} e^{ik(\psi_1(x)+\psi_2(x)-\ell)} dx. \quad (10)$$

The quantity of interest is the mean power gain relative to free space, i.e., the variance

$$\begin{aligned} V^2 &= \mathcal{E}\{|v_s|^2\} \\ &= \frac{k^4\ell^2}{4\pi^2} \iint g_1(x)g_1^*(x')g_2(x)g_2^*(x') \\ &\quad \cdot \frac{1}{r_1r_1'r_2r_2'} \exp[ik(\psi_1(x) - \psi_1(x') + \psi_2(x) - \psi_2(x'))] \\ &\quad \cdot R(x, x') dx dx' \end{aligned} \quad (11)$$

where $R(x, x') = \mathcal{E}\{\epsilon(x)\epsilon(x')\}$ is the refractivity-deviation autocorrelation function.

To make progress, various approximations and notational changes are introduced. The atmosphere is not statistically homogeneous, so it is useful to describe the autocorrelation function as depending on the point x and a “deviation” from that point $\rho = x' - x$, whence, R becomes $R(x, \rho)$. The notion is that the refractivity deviations $\epsilon(x)$ and $\epsilon(x')$ become rapidly independent as ρ increases so that R goes rapidly to zero for even moderately large ρ . Since only small values of ρ are important, it is assumed that within the integral we can set $g_i(x') = g_i(x + \rho) \approx g_i(x)$ and $r_i' \approx r_i$. Similarly, the phases are approximated as

$$\psi_i(x) - \psi_i(x') \approx \nabla\psi_i \cdot (x' - x) = p_i \cdot \rho \quad (12)$$

where $p_i(x) = \nabla\psi_i(x)$ are vectors tangent to the respective rays (see Figure 1). We then have

$$\begin{aligned} V^2 &= \frac{k^4 \ell^2}{4\pi^2} \iint |g_1(x)|^2 |g_2(x)|^2 \frac{1}{r_1^2 r_2^2} e^{ik(p_1+p_2)\cdot\rho} R(x, \rho) dx d\rho \\ &= \frac{k^4 \ell^2}{4\pi^2} \int |g_1(x)|^2 |g_2(x)|^2 \frac{1}{r_1^2 r_2^2} \Phi(x, k(p_1 + p_2)) dx \end{aligned} \quad (13)$$

where the integrand now includes the power spectral density

$$\Phi(x, \kappa) = \int e^{i\kappa\cdot\rho} R(x, \rho) d\rho \quad (14)$$

with $\kappa = k(p_1 + p_2)$.

A realistic description of the function Φ (or R) is required for further development of the theory. This depends on the behavior of the atmosphere at high altitudes and as noted by Dr. Hufford, it is a meteorological question, where the physical answer, while continuing to improve, is still somewhat in dispute. Continuing on, we will describe various approximations that lead to the forward scatter attenuation functions found in [2, 3, 5].

To make the problem tractable, two important assumptions are applied that purportedly provide answers considered to be close enough to the truth. For a particular point in the common volume, the power spectral density function describes the ‘‘spectrum’’ of dielectric irregularities (aka ‘‘blobs’’). The first assumption is that while the strength of the scattering due to the blobs varies in space, the ‘‘shape of the spectrum’’ stays about the same, hence, the variables can be separated, i.e., $\Phi(x, \kappa) = S(x)\Phi(\kappa)$ and also $R(x, \rho) = S(x)R(\rho)$. The second assumption is that the turbulence is isotropic so that R only depends on the length of ρ and not on the direction; this implies that Φ is a function of the length of κ alone.

The function $\Phi(\kappa)$ is the spectrum arising from homogeneous isotropic turbulence. A useful mathematical description of such spectra is the von Karmen series

$$\Phi(\kappa) = \frac{\sigma^2 \ell_0^3}{(1 + \kappa^2 \ell_0^2)^{\nu+3/2}} \quad (15)$$

where σ^2 determines the strength of the turbulence and ℓ_0 is the scale length or average size of the blobs. The inverse Fourier transform is the correlation function

$$R(\rho) = \sigma^2 \left(\frac{\rho}{2\ell_0} \right)^\nu \frac{\sqrt{\pi}}{\Gamma(\nu+3/2)} K_\nu \left(\frac{\rho}{\ell_0} \right) \quad (16)$$

where K_ν is the modified Bessel function.

This general formulation describes the various turbulence theories that were considered by researchers [1]. Setting $\nu = 1/2$ yields the original Booker-Gordon theory with correlation function $R(\rho) = (\pi\sigma^2/2)e^{-\rho/\ell_0}$. Obukhov and Kolmogoroff developed a turbulence model that says $\nu = 1/3$. Then there is the *mixing-in-gradient* model where $\nu = 1$. That model considers an initial

refractivity gradient and modifications due to turbulent convection over the entire spectrum. The obvious question: which model gives results that are in good agreement with measured data? This was answered by examining forward scatter radio-frequency dependence.

The frequency dependence for the various turbulence theories is easily estimated by considering terms in V^2 that directly involve the propagation constant k , viz.

$$V^2 \propto k^4 \Phi(k \dots) \propto \frac{k^4}{k^{2\nu+3}} = k^{1-2\nu}; \quad (17)$$

The Booker-Gordon model predicts that gain is independent of frequency, k^0 . According to the Obukhov-Kolmogoroff model, gain is proportional to $k^{1/3}$, i.e., scattered power increases with frequency. The mixing-in-gradient model yields power gain that is proportional to k^{-1} . According to [1], “this [mixing-in-gradient model] was found to be in good agreement with careful analysis of the data from numerous broad-beam experiments when the role of height gain factors is carefully included,” hence, that was determined to be the appropriate turbulence model.

A further simplification is obtained by assuming that κ is large. According to Dr. Hufford the justification for this is that

the minimum scatter angle within the common volume is that at the cross-over where the two horizon rays intersect. By the very nature of the problem this cannot be very small ...

yielding

$$\Phi(x, \kappa) = \frac{S(x)}{\kappa^5} \quad (18)$$

where the function S has been modified to include the constants described above. Evidently, based on radio measurements [1, 2], it is assumed that scattered signal power is proportional to the square of the mean gradient of the refractive index. Hence, scattering efficiency decreases exponentially with height above the horizon ray cross-over point, i.e.,

$$S(x) = S_0 e^{-2\gamma z} \quad (19)$$

where S_0 is the scattering efficiency at the cross-over point, and z is the elevation above the cross-over point.

The vectors p_i have length equal to the index of refraction $1 + \bar{N}$; since $1 \gg \bar{N}$, the length is assumed equal to 1. We then have $|p_1 + p_2| = 2 \sin \theta / 2$, where θ is the external angle between the vectors and it is also the angle between the ray coming from the transmitter and the ray going to the receiver; aka the scattering angle.

What about the gain functions g_i ? It is assumed that $g_i(x) = 0$ whenever x is below that terminal's horizon. Hence, the integrand is non-zero in the region above the intersection of the horizon rays, i.e., the common volume. In that region, it is assumed that the *incident* field is dominated by a

direct ray plus a ground reflected ray with reflection coefficient of -1 [7]. In terms of the *effective* antenna heights h_{ei} and what are called *elevation angles above the horizontal*, ψ_i , the gains are

$$g_i(x) = 1 - e^{i2kh_{ei}\sin\psi_i}, \quad |g_i|^2 = 4\sin^2 kh_{ei}\sin\psi_i. \quad (20)$$

The phrase used to describe the angles ψ_i is somewhat vague. In [7], they are called grazing angles. There we find that Figure 36 and Equation 45 provide a detailed description of the gain functions; the ψ_i are described as the angles between the horizon rays and the corresponding direct ray to a volume element within the common volume. The gain functions are further described as “the usual expressions for ground reflection lobery over a plane reflecting surface.” Referring to [3], the idea is that as the effective antenna heights, measured in wavelengths, become smaller, the direct and reflected wave energy tends to cancel at the lower part of the common volume, where *scattering efficiency is greatest*. Since it is the lower portion of the scattering volume that is important, the approximations associated with small grazing angles are perhaps reasonable. When kh_{ei} is large, there are many oscillations within small intervals of the grazing angles, so the \sin^2 terms can be replaced by $1/2$. For that case, the power is doubled on both the transmitter and receiver side.

With all of this, in principle, tropospheric scatter gain can be calculated via the following equation:

$$V^2 = \frac{4\ell^2}{\pi^2 k} \int_{\nu} \sin^2(kh_{e1}\sin\psi_1) \sin^2(kh_{e2}\sin\psi_2) \frac{1}{r_1^2 r_2^2} \frac{S_0 e^{-2\gamma z}}{(2\sin\theta/2)^5} dx. \quad (21)$$

where S_0 is the scattering efficiency at the cross-over point, and z is the elevation *above* that cross-over point. The common volume and variables are, as noted by Dr. Hufford, “well defined and easily pictured functions of the position vector x ”. The empirical constants S_0 and γ , depend on surface refractivity, and the height above the surface of the common volume cross-over point. Expressions that are used to calculate values for these *empirical* constants can be found in [3, 5].

In order to compare theoretical results with propagation model algorithms we need to evaluate the Common Volume Integral (21). As it stands, the integral, is still too difficult for practical calculations. The integrand is usually simplified via a host of geometric approximations. In what follows, we describe the methods we used to obtain solutions.

3 EVALUATION OF THE COMMON VOLUME INTEGRAL

We will use the coordinate systems and many of the geometric approximations defined in [7] (*Norton's geometry* shown in Figure 1) to improve tractability of the Common Volume Integral. The use of these approximations is justified, to some extent, in [8] (second column page 1345). Note that S_0 , defined above, is the scattering efficiency assuming that the coordinate system origin is at the cross-over point ($x = 0, z = h_0$ in Figure 1). For the coordinates defined by Figure 1, the scattering efficiency term is then $e^{2\gamma h_0} S_0$. In addition, we set $\rho_{1,2} = 2kh_{e1,2}$, $\eta = \gamma\theta/2$, $\rho_{1,2} = \rho_{1,2}\theta$, where $h_{e1,2}$ are effective antenna heights and γ is the logarithmic gradient of refractivity (see also [5]).

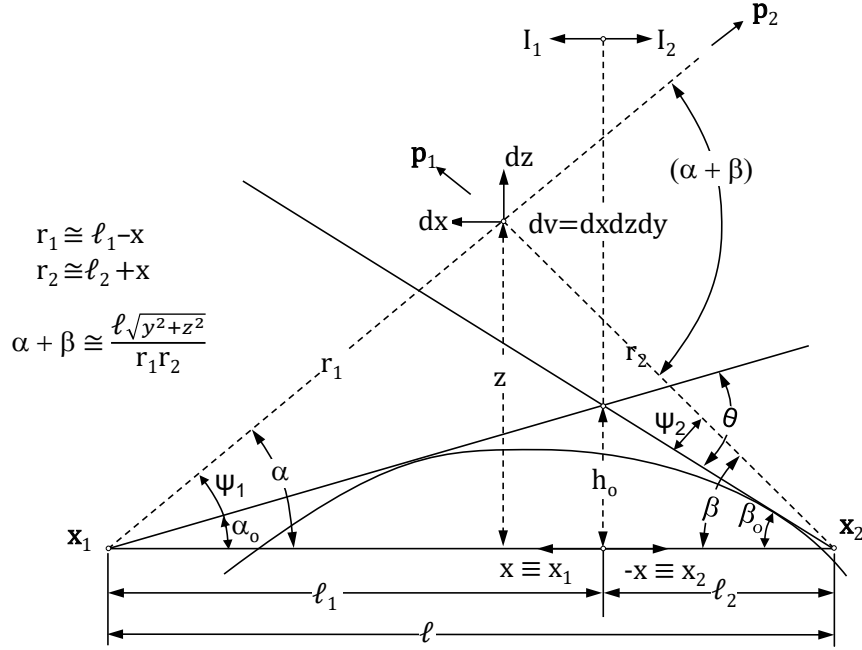


Figure 1. Geometry for the scatter integral

Applying Norton's geometry on the left side (I_1 in Figure 1) of the crossover point we obtain

$$V_L^2 = \frac{\ell^2 S_0 e^{2\gamma h_0}}{\pi^2 k} \int_0^{\ell_1} \int_{\beta_0(\ell_2+x)}^{\infty} \int_{-\infty}^{\infty} \frac{4g_t g_r (\ell_1 - x)^3 (\ell_2 + x)^3}{\ell^5 (y^2 + z^2)^{5/2}} e^{-2\gamma z} dy dz dx, \quad (22)$$

where according to Norton's geometrical approximation $g_t = \sin^2[kh_{e1}\psi_1]$ and $g_r = \sin^2[kh_{e2}\psi_2]$.

The integral over y is not difficult; we then have

$$V_L^2 = \frac{4 S_0 e^{2\gamma h_0}}{3 \pi^2 \ell^3 k} \int_0^{\ell_1} \int_{\beta_0(\ell_2+x)}^{\infty} \frac{(4g_t g_r) (\ell_1 - x)^3 (\ell_2 + x)^3 e^{-2\gamma z}}{z^4} dz dx. \quad (23)$$

Applying Norton's geometry to the product of the *gain* functions yields

$$4g_t g_r = 1 - \cos \rho_1 \psi_1 - \cos \rho_2 \psi_2 + (\cos(\rho_1 \psi_1 + \rho_2 \psi_2) + \cos(\rho_1 \psi_1 - \rho_2 \psi_2))/2, \quad (24)$$

where $\psi_1 = z/(\ell_1 - x) - \alpha_0$ and $\psi_2 = z/(\ell_2 + x) - \beta_0$. To obtain the volume integral on right hand side, make the following changes: $\beta_0 \rightarrow \alpha_0$, $\ell_2 \rightarrow \ell_1$, and $\ell_1 \rightarrow \ell_2$ except for the gain functions where $\psi_1 = z/(\ell_1 + x) - \alpha_0$ and $\psi_2 = z/(\ell_2 - x) - \beta_0$.

With this, the left and right volume integrals explode into many integrals; the details are given in Appendix A. Each of the integrals can be written in the following general form

$$\int_{\mu\ell}^{\ell} (\ell - w)^3 E_4(f(w)) dw = \int_{\mu\ell}^{\ell} (\ell - w)^3 f^3(w) \Gamma(-3, f(w)) dw \quad (25)$$

where

$$f(w) = \kappa w + \nu w/(\ell - w) + \lambda = -\kappa(\ell - w) + \nu\ell/(\ell - w) + \kappa\ell - \nu + \lambda; \quad (26)$$

κ , ν , and λ are constants that depend on the integral under consideration.

Four of these integrals (I_0 and one each for $I_{t,r}$) have "analytic" solutions. The rest are difficult and in our view require *numerical analysis*.

3.1 Analytic Solutions

When $\nu = 0$, there are relatively straightforward (although messy) analytic solutions. In this case,

$$\mathfrak{J} = \int_{\mu\ell}^{\ell} (\ell - w)^3 f^3(w) \Gamma(-3, f(w)) dw = \frac{1}{\kappa^4} \int_{\kappa\mu\ell+\lambda}^{\kappa\ell+\lambda} (\kappa\ell + \lambda - w)^3 w^3 \Gamma(-3, w) dw \quad (27)$$

$$= \frac{1}{\kappa^4} \sum_{n=0}^3 (-1)^n \binom{3}{n} (\kappa\ell + \lambda)^{3-n} \int_{\kappa\mu\ell+\lambda}^{\kappa\ell+\lambda} w^{3+n} \Gamma(-3, w) dw. \quad (28)$$

Applying partial integration, we see that

$$\int w^{n+3} \Gamma(-3, w) dw = \frac{1}{n+4} [w^{n+4} \Gamma(-3, w) - \Gamma(n+1, w)], \quad (29)$$

and, setting $a_n = 140(-1)^n \binom{3}{n} / (n+4)$, we obtain

$$\mathfrak{J} = \frac{1}{140\kappa^4} \sum_{n=0}^3 a_n (\kappa\ell + \lambda)^{3-n} [w^{n+4} \Gamma(-3, w) - \Gamma(n+1, w)] \Big|_{\kappa\mu\ell+\lambda}^{\kappa\ell+\lambda}. \quad (30)$$

We then have

$$\mathfrak{J} = \frac{\mathfrak{J}_u - \mathfrak{J}_\ell}{140\kappa^4} \quad (31)$$

where

$$\mathfrak{J}_u = (\kappa\ell + \lambda)^4 \mathbf{E}_4(\kappa\ell + \lambda) - \sum_{n=0}^3 a_n (\kappa\ell + \lambda)^{3-n} \Gamma(n+1, \kappa\ell + \lambda) \quad (32)$$

$$\begin{aligned} \mathfrak{J}_\ell &= (\kappa\ell + \lambda)^3 (\kappa\mu\ell + \lambda)^4 \Gamma(-3, \kappa\mu\ell + \lambda) \sum_{n=0}^3 a_n \left[\frac{\kappa\mu\ell + \lambda}{\kappa\ell + \lambda} \right]^n - \\ &\quad \sum_{n=0}^3 a_n (\kappa\ell + \lambda)^{3-n} \Gamma(n+1, \kappa\mu\ell + \lambda) \end{aligned} \quad (33)$$

$$\begin{aligned} \mathfrak{J}_\ell &= (\kappa\ell + \lambda)^3 (\kappa\mu\ell + \lambda) \mathbf{E}_4(\kappa\mu\ell + \lambda) \sum_{n=0}^3 a_n \left[\frac{\kappa\mu\ell + \lambda}{\kappa\ell + \lambda} \right]^n - \\ &\quad \sum_{n=0}^3 a_n (\kappa\ell + \lambda)^{3-n} \Gamma(n+1, \kappa\mu\ell + \lambda); \end{aligned} \quad (34)$$

note that $a_0 = 35$, $a_1 = -84$, $a_2 = 70$, $a_3 = -20$, so $\sum_{n=0}^3 a_n = 1$.

Ultimately, we are interested in parameter studies; hence, we find it useful to describe the foregoing results as functions of the various parameters:

$$\mathfrak{J}(\kappa, \lambda, \mu) = \frac{\mathfrak{J}_u(\kappa, \lambda) - \mathfrak{J}_\ell(\kappa, \lambda, \mu)}{140\kappa^4}. \quad (35)$$

3.2 Numerical Solutions

When $\nu \neq 0$, the integrand is highly oscillatory, and in our view numerical analysis like that described here must be used. For these integrals, we use the notation

$$\mathcal{I} = \int_{\mu\ell}^{\ell} (\ell - w)^3 \mathbf{E}_4(f(w)) dw \quad (36)$$

and define $A = -\kappa$, $B = \kappa\ell - \nu + \lambda$, and $C = \nu\ell$ so that we can write

$$f(w) = A(\ell - w) + B + C/(\ell - w) = A\ell(1 - w/\ell) + \frac{C}{\ell(1 - w/\ell)} + B. \quad (37)$$

Setting $y = 1 - w/\ell$ we obtain

$$\mathcal{I} = \ell^4 \int_0^{1-\mu} y^3 \mathbf{E}_4(g(y)) dy, \quad g(y) = A\ell y + \frac{C}{\ell y} + B. \quad (38)$$

Noting that the generalized exponential integral can be written as a continued fraction, viz.

$$E_n(z) = e^{-z} \left(\frac{1}{z+} \frac{n}{1+z+} \frac{1}{1+} \frac{n+1}{1+} \frac{2}{z+} \dots \right) \quad (|\arg z| < \pi), \quad (39)$$

we see that it can be cast in terms of the product of an oscillatory term $e^{-i\text{Im}z}$ and a non oscillatory-term $e^{i\text{Im}z} E_n(z)$ that can be well approximated by a polynomial.

3.2.1 Polynomial Approximation

Referring to the previous equation, the function of interest is

$$F(y) = y^3 e^{\frac{C}{\ell y}} E_4(g(y)) \quad (40)$$

where

$$\frac{\mathcal{I}}{\ell^4} = \int_0^{1-\mu} F(y) e^{\frac{-C}{\ell y}} dy. \quad (41)$$

The idea is to divide the integral into a sum of several integrals over equal subintervals. Lagrangian 3-point interpolation is applied to $F(y)$ on each subinterval yielding a second degree polynomial approximation. Each term of the polynomial is integrated against the wildly oscillating complex exponential yielding

$$\int y^k e^{\frac{-C}{\ell y}} dy = y^{k+1} E_{k+2} \left(\frac{C}{\ell y} \right) \quad k = 0, 1, 2. \quad (42)$$

In what follows, we will use standard difference operator notation, viz.

$$\begin{aligned} \Delta F_k &= F_{k+1} - F_k \\ \Delta^2 F_k &= \Delta(\Delta F_k) = F_{k+2} - 2F_{k+1} + F_k. \end{aligned}$$

3.2.2 Interpolation

There are M subintervals, each has a length $2h = \frac{1-\mu}{M}$. Setting $y_j = jh$ and $F_j = F(y_j)$, the interpolation polynomial for the m^{th} interval is

$$F^{(m)}(y) = \frac{p(p-1)}{2} F_{2m-2} + (1-p^2) F_{2m-1} + \frac{p(p+1)}{2} F_{2m}, \quad m = 1, \dots, M \quad (43)$$

where $p = (y - y_{2m-1})/h$.

It seems useful to manipulate this into a simple power series as follows:

$$F^{(m)}(y) = \frac{(y - y_{2m-1})^2}{2h^2} \Delta^2 F_{2m-2} + \frac{y - y_{2m-1}}{2h} (F_{2m} - F_{2m-2}) + F_{2m-1} \quad (44)$$

$$\begin{aligned} &= \frac{y^2}{2h^2} \Delta^2 F_{2m-2} + y \left(\frac{F_{2m} - F_{2m-2}}{2h} - \frac{y_{2m-1} \Delta^2 F_{2m-2}}{h^2} \right) + \\ &F_{2m-1} + \frac{y_{2m-1}^2}{2h^2} \Delta^2 F_{2m-2} - \frac{y_{2m-1}}{2h} (F_{2m} - F_{2m-2}); \end{aligned} \quad (45)$$

then define coefficients:

$$c_m^{(2)} = \frac{\Delta^2 F_{2m-2}}{2h^2} \quad (46)$$

$$c_m^{(1)} = \frac{F_{2m} - F_{2m-2}}{2h} - 2y_{2m-1} c_m^{(2)} \quad (47)$$

$$c_m^{(0)} = F_{2m-1} - y_{2m-1} \left(c_m^{(1)} + y_{2m-1} c_m^{(2)} \right), \quad (48)$$

yielding

$$F^{(m)}(y) = \begin{cases} \sum_{k=0}^2 c_m^{(k)} y^k & 2(m-1) \leq y/h \leq 2m \\ 0 & \text{else} \end{cases} \quad (49)$$

3.3 The Numerical Integration Algorithm

The integral can then be *approximated* as

$$\frac{\mathcal{J}}{\ell^4} = \int_0^{1-\mu} \sum_{m=1}^M F^{(m)}(y) e^{\varpi/y} dy = \sum_{m=1}^M \int_{2(m-1)h}^{2mh} \sum_{k=0}^2 c_m^{(k)} y^k e^{\varpi/y} dy, \quad (50)$$

and hence,

$$\frac{\mathcal{J}}{\ell^4} = \sum_{m=1}^M \sum_{k=0}^2 c_m^{(k)} \left[(2mh)^{k+1} E_{k+2} \left(-\frac{\varpi}{2mh} \right) - (2(m-1)h)^{k+1} E_{k+2} \left(-\frac{\varpi}{2(m-1)h} \right) \right]. \quad (51)$$

Note that $E_n(\infty) = 0$ so that the lower limits when $m = 1$ are zero. Also note that, except for the coefficients, the upper limit of the m^{th} term is the same as the lower limit of the $(m+1)^{\text{th}}$ term. We then have

$$\frac{\mathcal{J}}{\ell^4} = \sum_{k=0}^2 \left[\sum_{m=1}^{M-1} -\Delta c_m^{(k)} (2mh)^{k+1} E_{k+2} \left(-\frac{\varpi}{2mh} \right) + c_M^{(k)} (2Mh)^{k+1} E_{k+2} \left(-\frac{\varpi}{2Mh} \right) \right] \quad (52)$$

where $\Delta c_m^{(k)} = c_{m+1}^{(k)} - c_m^{(k)}$, $\varpi = -C/\ell$, $2Mh = 1 - \mu$, and $h = \frac{1-\mu}{2M}$.

Note that these results are actually functions of $(A\ell, B, C/\ell)$, i.e., the dependence on ℓ is only via $2\eta = \gamma\theta\ell$; hence, parameter studies will not explicitly depend on ℓ .

3.4 A Formal Result

In this section we devise a *formal* expression for the whole mess, i.e., V^2 . To this end, we will concoct notation for the various parameters to obtain a somewhat compact expression for V^2 . Since each integral has a different set of parameters, we will sort this out by using superscripts and subscripts to tie them to the various integrals.

For each $I_{t,r}$ and $I_{t\pm r}$ (see (A-13)-(A-16)), there are two integrals. Parameters belonging to the first integral will be denoted with the superscript (1) and parameters belonging to the second integral will be denoted with the superscript (2). The parameters μ and κ have two values

$$\begin{aligned} \mu^{(1)} &= (1-s)/2, \quad \mu^{(2)} = (1+s)/2, \\ \kappa^{(1)} &= \gamma\theta(1+s), \quad \kappa^{(2)} = \gamma\theta(1-s) \end{aligned}$$

where s is the modulus of asymmetry (see [5] and Appendix A).

As an example of this scheme, we can at this point, construct the formal expression for I_0 , viz.

$$I_0 = \frac{8\ell^4}{140\theta^3} \left[\frac{\mathfrak{J}_u(\kappa^{(1)}, \lambda_0^{(1)}) - \mathfrak{J}_\ell(\kappa^{(1)}, \mu^{(1)}, \lambda_0^{(1)})}{[\kappa^{(1)}\ell]^4(1+s)^3} + \frac{\mathfrak{J}_u(\kappa^{(2)}, \lambda_0^{(2)}) - \mathfrak{J}_\ell(\kappa^{(2)}, \mu^{(2)}, \lambda_0^{(2)})}{[\kappa^{(2)}\ell]^4(1-s)^3} \right] \quad (53)$$

where $\lambda_0^{(j)} = 0$, and I_0 , \mathfrak{J}_u and \mathfrak{J}_ℓ are defined by (A-13), (33), and (34).

The parameters \mathbf{v} and λ also depend on the particular term, i.e., $I_{t,r}$ or $I_{t\pm r}$, so we will use subscripts to keep track of that as necessary; then for \mathbf{v} ,

$$\begin{aligned} v_t^{(1)} &= -i\rho_1(1+s)/2, \quad v_t^{(2)} = 0, \quad v_r^{(1)} = 0, \quad v_r^{(2)} = -i\rho_2(1-s)/2, \\ v_{t+r}^{(1)} &= -i\rho_1(1+s)/2, \quad v_{t+r}^{(2)} = -i\rho_2(1-s)/2, \\ v_{t-r}^{(1)} &= -i\rho_1(1+s)/2, \quad v_{t-r}^{(2)} = i\rho_2(1-s)/2, \end{aligned}$$

and for λ ,

$$\begin{aligned} \lambda_t^{(1)} &= 0, \quad \lambda_t^{(2)} = -i\rho_1(1-s)/2, \quad \lambda_r^{(1)} = -i\rho_2(1+s)/2, \quad \lambda_r^{(2)} = 0, \\ \lambda_{t+r}^{(1)} &= -i\rho_2(1+s)/2, \quad \lambda_{t+r}^{(2)} = -i\rho_1(1-s)/2, \\ \lambda_{t-r}^{(1)} &= i\rho_2(1+s)/2, \quad \lambda_{t-r}^{(2)} = -i\rho_1(1-s)/2. \end{aligned}$$

If we do the same sort of thing for the parameters A , B , and C , we find

$$\begin{aligned} A^{(1)} &= -2\eta(1+s)/\ell, \quad A^{(2)} = -2\eta(1-s)/\ell \\ B_t^{(1)} &= 2\eta(1+s) \left[1 + \frac{i\rho_1}{4\eta} \right], \quad B_t^{(2)} = n/a, \quad B_r^{(1)} = n/a, \quad B_r^{(2)} = 2\eta(1-s) \left[1 + \frac{i\rho_2}{4\eta} \right], \\ B_{t+r}^{(1)} &= 2\eta(1+s) \left[1 + \frac{i(\rho_1 - \rho_2)}{4\eta} \right], \quad B_{t+r}^{(2)} = 2\eta(1-s) \left[1 + \frac{i(\rho_2 - \rho_1)}{4\eta} \right], \\ B_{t-r}^{(1)} &= 2\eta(1+s) \left[1 + \frac{i(\rho_1 + \rho_2)}{4\eta} \right], \quad B_{t-r}^{(2)} = 2\eta(1-s) \left[1 - \frac{i(\rho_1 + \rho_2)}{4\eta} \right], \\ C^{(1)} &= -\frac{i\rho_1\ell(1+s)}{2}, \quad C^{(2)} = -C^{*(2)} = -\frac{i\rho_2\ell(1-s)}{2} \end{aligned}$$

Then formally we can write

$$I_t = \frac{8\ell^4}{\theta^3} \operatorname{Re} \left\{ e^{-i\rho_1 \frac{1+s}{2}} \left[\frac{\mathcal{I}(A^{(1)}, B_t^{(1)}, C^{(1)}, \mu^{(1)})}{\ell^4(1+s)^3} + \frac{\mathfrak{J}_u(\kappa^{(2)}, \lambda_t^{(2)}) - \mathfrak{J}_\ell(\kappa^{(2)}, \mu^{(2)}, \lambda_t^{(2)})}{140[\kappa^{(2)}\ell]^4(1-s)^3} \right] \right\} \quad (54)$$

$$I_r = \frac{8\ell^4}{\theta^3} \operatorname{Re} \left\{ e^{-i\rho_2 \frac{1+s}{2}} \left[\frac{\mathfrak{J}_u(\kappa^{(1)}, \lambda_r^{(1)}) - \mathfrak{J}_\ell(\kappa^{(1)}, \mu^{(1)}, \lambda_r^{(1)})}{140[\kappa^{(1)}\ell]^4(1+s)^3} + \frac{\mathcal{I}(A^{(2)}, B_r^{(2)}, C^{(2)}, \mu^{(2)})}{\ell^4(1-s)^3} \right] \right\} \quad (55)$$

$$I_{t+r} = \frac{8\ell^4}{\theta^3} \operatorname{Re} \left\{ e^{-i(\rho_1 \frac{1-s}{2} + \rho_2 \frac{1+s}{2})} \left[\frac{\mathcal{I} \left(A^{(1)}, B_{t+r}^{(1)}, C^{(1)}, \mu^{(1)} \right)}{\ell^4 (1+s)^3} + \frac{\mathcal{I} \left(A^{(2)}, B_{t+r}^{(2)}, C^{(2)}, \mu^{(2)} \right)}{\ell^4 (1-s)^3} \right] \right\} \quad (56)$$

$$I_{t-r} = \frac{8\ell^4}{\theta^3} \operatorname{Re} \left\{ e^{-i(\rho_1 \frac{1-s}{2} - \rho_2 \frac{1+s}{2})} \left[\frac{\mathcal{I} \left(A^{(1)}, B_{t-r}^{(1)}, C^{(1)}, \mu^{(1)} \right)}{\ell^4 (1+s)^3} + \frac{\mathcal{I} \left(A^{(2)}, B_{t-r}^{(2)}, C^{*(2)}, \mu^{(2)} \right)}{\ell^4 (1-s)^3} \right] \right\} \quad (57)$$

This combined with

$$V^2 = \left[\frac{4}{3\pi^2} S_0 \right] e^{2\gamma h_0} \left(\frac{\ell}{\theta^3 k} \right) \frac{\theta^3}{\ell^4} [I_0 - I_t - I_r + (I_{t+r} + I_{t-r})/2] \quad (58)$$

is used to calculate transmission gain. The transmission attenuation (preferred by engineers) is the reciprocal, in decibels i.e., $-10 \log V^2$.

4 THEORY VS. PROPAGATION MODELS

In this section, we compare theoretical results obtained from the Common Volume Integral with those obtained from the Irregular Terrain Model (ITM) and IF-77 Electromagnetic Wave propagation model (IF-77) [4, 5]. For this, it is convenient to describe forward scatter attenuation in terms of the *frequency gain function* H_0 viz.

$$A_s = -10 \log \left[\frac{4}{3\pi} S_0 e^{2\gamma h_0} \right] + 10 \log \left(\frac{\theta^3 k}{\ell} \right) - 10 \log \left(\frac{\theta^3 I_0}{\ell^4} \right) + H_0 \quad (59)$$

where

$$H_0 = -10 \log \left[1 - \frac{I_t + I_r}{I_0} + \frac{I_{t+r} + I_{t-r}}{2I_0} \right]. \quad (60)$$

It is assumed that if the antennas, measured in wavelengths, are sufficiently high, reflection of energy by the ground doubles the power incident on scatterers and again doubles the power scattered to the receiver. For that case H_0 is negligible. As the frequency is reduced, effective antenna heights in wavelengths become smaller, and ground-reflected energy tends to cancel direct-ray energy at the lower part of the common volume where scattering efficiency is greatest. Then H_0 provides an estimate of the corresponding increase in attenuation.

Calculating attenuation when H_0 can be neglected is tedious but rather straightforward. That is also true for the case of constant refractivity even when H_0 cannot be neglected. Comparisons with propagation models for those cases will be examined first. When the refractivity is not constant numerical analysis of the Common Volume Integral is required. For those cases, we will compare theoretical calculations of H_0 with model predictions.

4.1 Theory vs. Models When Frequency Gain Is Negligible

As described above, frequency gain is negligible when kh_{te} and kh_{re} are large so that, due to wild oscillations of the integrands, $I_{t,r}$ and $I_{t\pm r}$ are negligible; according to [7], this is the case when $\rho_{1,2} > 20$. We start with (53) and write $I_0 = \frac{\ell^4}{\theta^3} [L + R]$, $G = 2\mu^{(1)}$, $H = 2\mu^{(2)}$, and $\eta_s = 2(1 - s^2)\eta$. We then have

$$L = \frac{1}{H^3} \left\{ E_4 \left(\frac{\eta_s}{G} \right) - e^{-\eta_s/G} \frac{G}{\eta_s} \left[1 - 4 \frac{G}{\eta_s} + 20 \left(\frac{G}{\eta_s} \right)^2 - 120 \left(\frac{G}{\eta_s} \right)^3 \right] - \frac{G}{2} E_4 \left(\frac{\eta_s}{2} \right) \sum_{n=0}^3 a_n \left(\frac{G}{2} \right)^n - e^{\frac{\eta_s}{2}} \frac{G}{\eta_s} \left[\sum_{n=0}^3 a_n \left(\frac{G}{2} \right)^n + (a_1 G + a_2 G^2 + 3a_3 G^3/4)/\eta_s + (2a_2 G^2 + 3a_3 G^3)/\eta_s^2 + 6a_3 G^3/\eta_s^3 \right] \right\}, \quad (61)$$

R is obtained by replacing s with $-s$, i.e., interchanging G and H . The idea then is to obtain a polynomial fit to the function

$$\mathcal{Y}(\eta, s) = \left(\frac{\theta^3 I_0}{\ell^4} \right)^{-1}. \quad (62)$$

First, consider the limiting cases, viz. constant refractivity ($\eta \rightarrow 0$) and $\eta \rightarrow \infty$. For the former, we have (cf. Appendix A)

$$\begin{aligned} \int_0^{\ell_1} \int_{\beta_0(\ell_2+x)}^{\infty} \frac{(\ell_1-x)^3(\ell_2+x)^3}{z^4} dz dx &= \frac{\ell_1^4}{12\beta_0^3} \\ \int_0^{\ell_2} \int_{\alpha_0(\ell_1+x)}^{\infty} \frac{(\ell_2-x)^3(\ell_1+x)^3}{z^4} dz dx &= \frac{\ell_2^4}{12\alpha_0^3} \end{aligned} \quad (63)$$

Noting that $\beta_0/\ell_1 = \alpha_0/\ell_2 = \theta/\ell$ we obtain

$$I_0 = \frac{\ell^4}{\theta^3} \frac{1}{12}. \quad (64)$$

For large z

$$E_4(z) \sim \frac{e^{-z}}{z} \left[1 - \frac{4}{z} + \frac{20}{z^2} - \frac{120}{z^3} + \dots \right] \quad (65)$$

where we find that the terms related to the upper limit of the integral are negligible and after some tedious manipulations we find that $I_0 = 4\ell^4/(\theta^3\eta_s^2)$.

Considering the limiting cases we assume that the estimate has the form

$$\hat{\mathcal{Y}}(\eta, s, a, b, c) = ((1-s^2)\eta)^2 + (as^2 + bs + c)\eta + 12. \quad (66)$$

For $s = 0$, minimizing squared differences (least squares) yields $c = 8$. Since $\mathcal{Y}(\eta, s)$ is symmetric in s , $b = 0$. Then we set

$$\frac{\partial}{\partial a} \int_0^L \int_{-1}^1 [\mathcal{Y}(\eta, s) - \hat{\mathcal{Y}}(\eta, s, a)]^2 ds d\eta = 0. \quad (67)$$

The integration over s is easily performed via Gauss-Legendre quadrature and then we find that $a = 6$.

Finally, when $\rho_{1,2}$ are very large, the forward scatter attenuation can be described as

$$-20 \log V = -10 \log \left[\frac{4}{3\pi^2} S_0 e^{2\gamma h_0} \right] + 10 \log \left[((1-s^2)\eta)^2 + (6s^2 + 8)\eta + 12 \right] + \log(k\theta^3/\ell). \quad (68)$$

We see that the IF-77 Electromagnetic Wave Propagation Model uses exactly this result to calculate forward scatter attenuation ([5] Equation 220). We also see that the model's "scattering efficiency term" corresponds to $-10 \log \left[\frac{4}{3\pi^2} S_0 \right]$. We then have an explicit expression that describes the scattering efficiency function in terms of surface refractivity, refractivity gradient, and volume height. Based on our research, this is the only document we have located that provides a coherent expression for the scattering efficiency function used by the propagation models. Attenuation calculated using procedures described in Technical Note 101 [3] and ITM [4] are consistent with these results.

4.2 Frequency Gain for a Constant Refractive Index $\eta = 0$ and $\rho_{1,2} < \infty$

The integration, while doable, is tedious and details are given in the appendix. For this case, we find that

$$H_0 = -10 \log \left[\operatorname{Re} \left\{ 1 + \frac{3}{1 - \rho_2^2 / \rho_1^2} \left[\frac{\rho_2^2}{\rho_1^2} e^{-i\rho_1} E_4(-i\rho_1) - e^{-i\rho_2} E_4(-i\rho_2) \right] \right\} \right]; \quad (69)$$

obviously there is trouble when $\rho_1 = \rho_2 = \rho$. Taking the limit we obtain

$$H_0 = -10 \log \left[\operatorname{Re} \left\{ 1 + 3 e^{-i\rho} \left[\frac{i\rho}{2} E_3(-i\rho) - \left(1 + \frac{i\rho}{2} \right) E_4(-i\rho) \right] \right\} \right]. \quad (70)$$

To compare this with what is found in [3] requires some additional arithmetic. We will use (A-1) to put this result in terms of the sine and cosine integrals and related auxiliary functions defined by Equations III.50-51 [3]. Then for real ρ we find that

$$\operatorname{Re} \{ e^{-i\rho} E_4(-i\rho) \} = \frac{1}{6} [-\rho^2 + 2 - \rho^3 \operatorname{Re} \{ i e^{-i\rho} E_1(-i\rho) \}] \quad (71)$$

$$\operatorname{Re} \{ i e^{-i\rho} E_1(-i\rho) \} = - \left[\operatorname{Ci}(\rho) \sin \rho + \left(\frac{\pi}{2} - \operatorname{Si}(\rho) \right) \cos \rho \right] = -f(\rho) = -\frac{h(\rho)}{\rho} \quad (72)$$

and hence $\operatorname{Re} \{ e^{-i\rho} E_4(-i\rho) \} = [2 - \rho(1 - h(\rho))] / 6$. This is applied to (69) to obtain

$$h_0 = 10^{H_0/10} = \frac{2(1 - \rho_2^2 / \rho_1^2)}{\rho_2^2 (h(\rho_1) - h(\rho_2))}; \quad (73)$$

that is Equation III.49 [3].

Obviously this does not work for $\rho_1 = \rho_2$. For this case, set $\rho_2 = \rho_1 + \varepsilon$ and $\rho_1 = \rho$, then take the limit $\varepsilon \rightarrow 0$. We then have $h(\rho_2) \approx h(\rho_1) + h'(\rho_1)\varepsilon$ and to the first order in ε ,

$$h_0 = \frac{4}{\rho^3 h'(\rho)}. \quad (74)$$

We then use $h(\rho) = \rho f(\rho)$, $h'(\rho) = f(\rho) + \rho f'(\rho)$ and $f'(\rho) = g(\rho)$ where

$$g(\rho) = \operatorname{Ci}(\rho) \cos \rho - [\pi/2 - \operatorname{Si}(\rho)] \sin \rho \quad (75)$$

to obtain

$$h_0 = \frac{4}{\rho^3 [f(\rho) + \rho g(\rho)]} = \frac{4}{\rho^2 [h(\rho) + \rho^2 g(\rho)]} \quad (76)$$

a result that differs from Equation III.52 [3]. Note that $g(\rho)$ as defined here and [3] is “ $-g(\rho)$ ” as defined by Abramowitz and Stegun [11] (and also NIST Digital Library of Mathematical Functions <https://dlmf.nist.gov>).

4.2.1 Now For Some Curve Fitting

To start, we look at the curves obtained from (73) by assuming ρ_1 or ρ_2 is very large, viz.

$$h_0 = \frac{2}{\rho_2^2[1-h(\rho_2)]} \quad \rho_1 \gg \rho_2 \quad (77)$$

$$h_0 = \frac{2}{\rho_1^2[1-h(\rho_1)]} \quad \rho_2 \gg \rho_1. \quad (78)$$

Evidently, the idea is to fit

$$\zeta(\rho) = \frac{2}{1-h(\rho)}$$

with a quadratic function that is a perfect square (i.e., the vertex is on the ρ -axis). This is rather easy since for decreasing ρ , $h(\rho) \rightarrow 0$ and for large ρ $h(\rho) \sim 1 - 2/\rho^2$ yielding $\zeta(\rho) = (\rho + \sqrt{2})^2$. This gives pretty good results for moderate values of ρ when compared to rational approximations [11]. We then set $h(\rho) = 1 - 2/(\rho + \sqrt{2})^2$ and obtain

$$h(\rho_1) - h(\rho_2) = 2 \frac{(\rho_1 + \sqrt{2})^2 - (\rho_2 + \sqrt{2})^2}{(\rho_1 + \sqrt{2})^2(\rho_2 + \sqrt{2})^2} = 2 \frac{(\rho_1 - \rho_2)(\rho_1 + \rho_2 + 2\sqrt{2})}{(\rho_1 + \sqrt{2})^2(\rho_2 + \sqrt{2})^2}. \quad (79)$$

Inserting this into (73) we find

$$h_0 = \frac{(\rho_1 + \sqrt{2})^2(\rho_2 + \sqrt{2})^2}{\rho_1^2\rho_2^2} \left(\frac{\rho_1 + \rho_2}{\rho_1 + \rho_2 + 2\sqrt{2}} \right) \quad (80)$$

or

$$H_0(\rho_1, \rho_2, 0) = 10 \log \left[\left(1 + \frac{\sqrt{2}}{\rho_1} \right)^2 \left(1 + \frac{\sqrt{2}}{\rho_2} \right)^2 \frac{\rho_1 + \rho_2}{\rho_1 + \rho_2 + 2\sqrt{2}} \right]; \quad (81)$$

this is exactly what is found in the propagation model algorithms when $\eta = 0$ [4, 5].

Next, we will compare the theoretical and model frequency gain functions. Before continuing, it should be noted that when it comes to common volume asymmetry, ITM is quite limited. Evidently, referring to [4] and Figure 9.1 found in [3], ITM is limited to asymmetry factors no smaller than 3/4 and no larger than 5/4.

4.3 Theory vs. Models When Frequency Gain Is Not Negligible

Having established that the propagation models and theory are consistent when H_0 is negligible, we only need to compare theoretical calculations of H_0 with those generated by propagation models. The size of H_0 depends on the parameters $\rho_{1,2}$, η_s , and the *asymmetry factor* [4]

$$s_0 = \frac{1-s}{1+s} \quad (82)$$

where s is the IF-77 *modulus of asymmetry* [5].

The magnitude of the asymmetry factor plays a significant role in the determination of H_0 . Evidently, the ITM algorithm is limited to scatter volumes that are close to being symmetric ($s_0 = 1$). This is evidenced by the fact that the algorithm [4] uses Figure 9.1 of [3]. This leads us to consider the CCIR method for calculating H_0 that is described in [10]. That procedure was used by the 1973 air/ground propagation model (IF-73 [12]) that “evolved into” the IF-77 propagation model. CCIR data covers a wide range of parameters including highly asymmetric scattering volumes. For nearly symmetric scenarios, the ITM and CCIR methods are essentially the same; otherwise, ITM and CCIR methods appear to yield quite different results.

Our view is that ITM should be restricted to nearly symmetric forward scatter scenarios where there is agreement with CCIR. Hence, in what follows we need only compare the theoretical solution with the CCIR method and H_0 calculated via the IF-77 algorithm.

Since H_0 is a function of several parameters, a detailed comparison over the entire range of parameter values would require a significant effort. Our view is that if there is reasonable agreement between theory and the models over a subset of parameter values that include, for example, highly asymmetric volumes, it is reasonable to assume that the model algorithms are consistent with theory. Exact agreement is not expected since numerical evaluation of the volume integrals is somewhat tricky. The numerical methods used to obtain the CCIR data are unknown and that result was subjected to some sort of empirical curve fitting scheme.

Our view is that what is shown in the following figures reveals, for the most part, that theoretically generated data and CCIR data are fairly consistent, particularly considering that the CCIR data includes empirical curve fitting.

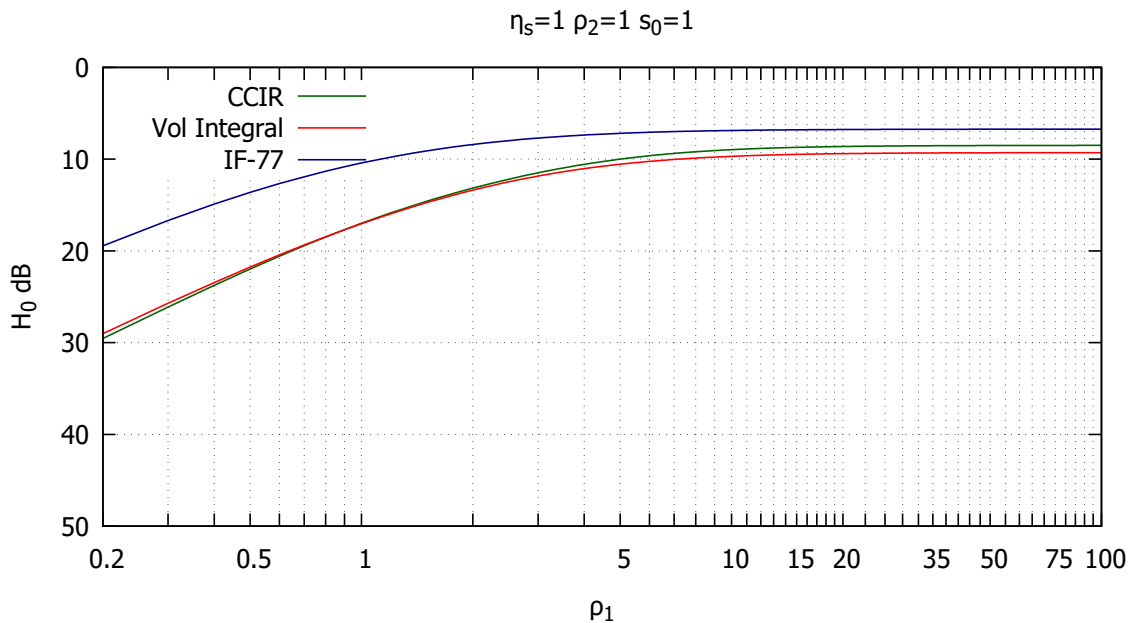


Figure 2. $\eta_s = 1$, asymmetry factor=1, $\rho_2 = 1$

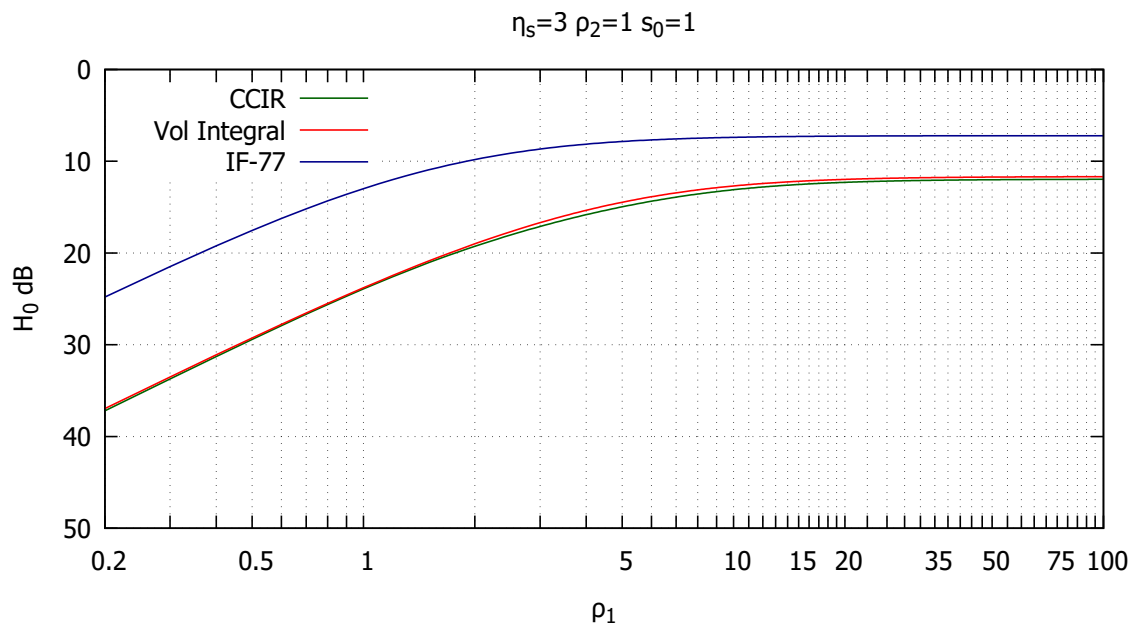


Figure 3. $\eta_s = 3$, asymmetry factor=1, $\rho_2 = 1$

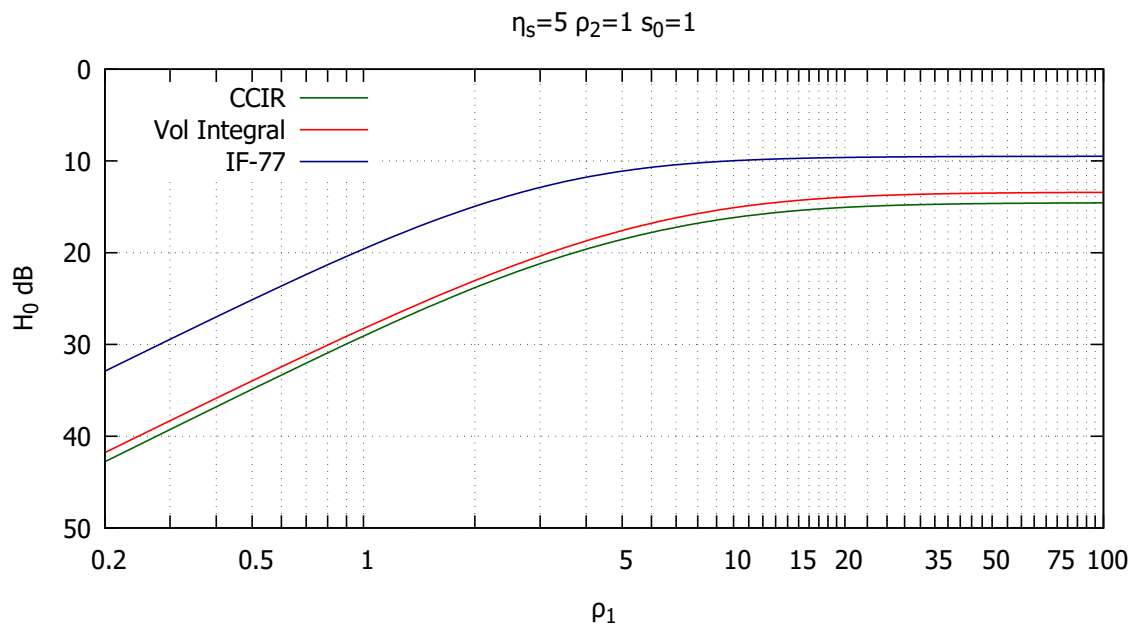


Figure 4. $\eta_s = 5$, asymmetry factor=1, $\rho_2 = 1$

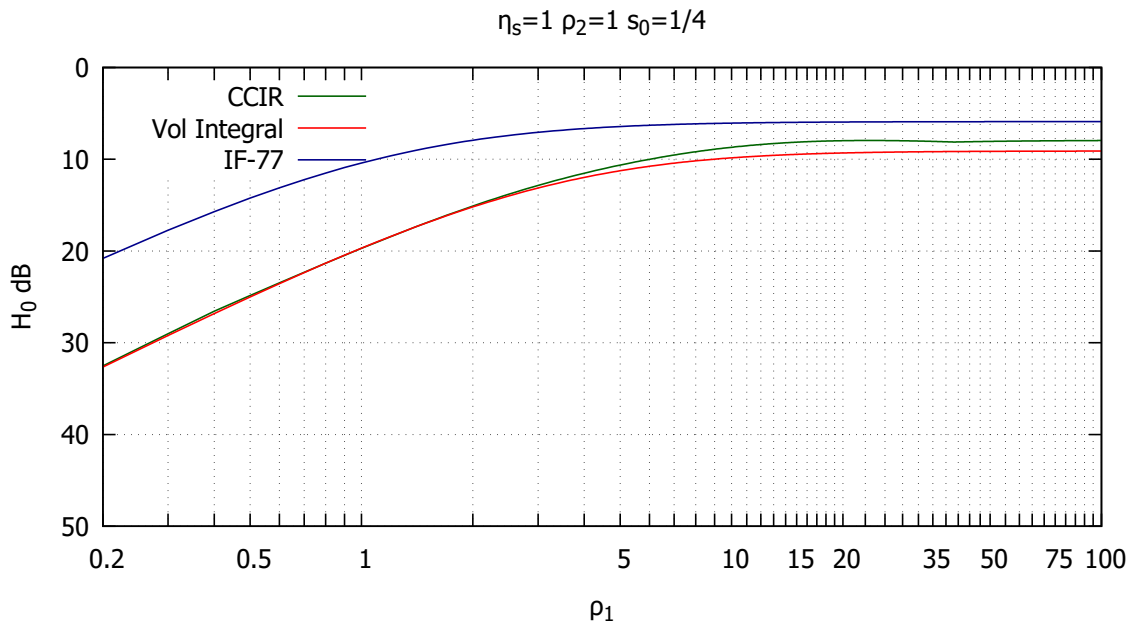


Figure 5. $\eta_s = 1$, asymmetry factor=1/4, $\rho_2 = 1$

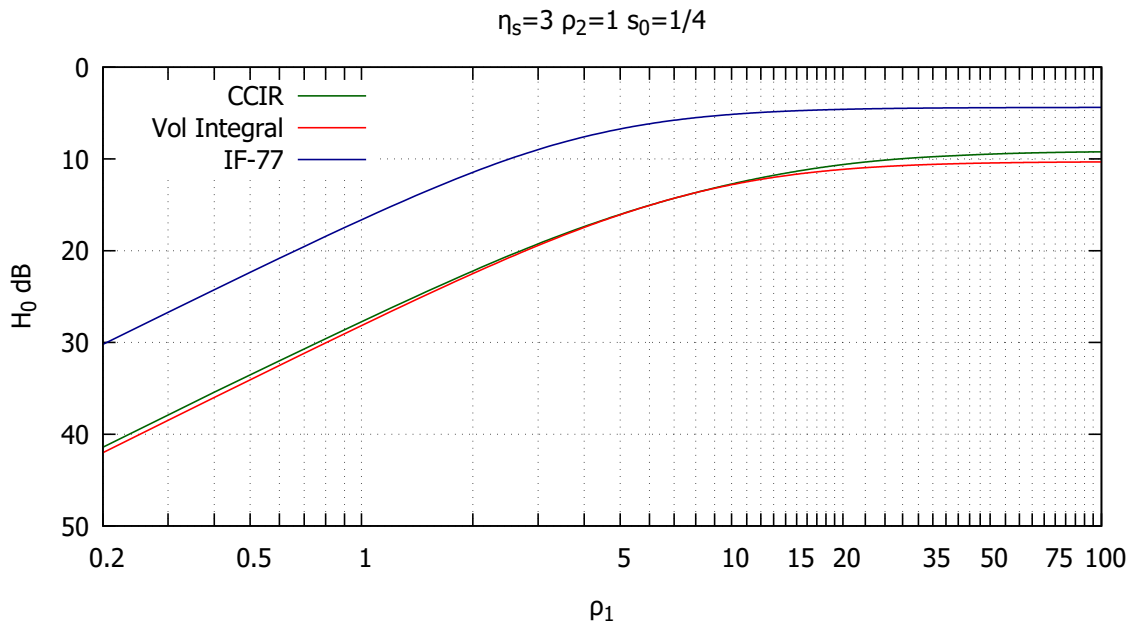


Figure 6. $\eta_s = 3$, asymmetry factor=1/4, $\rho_2 = 1$

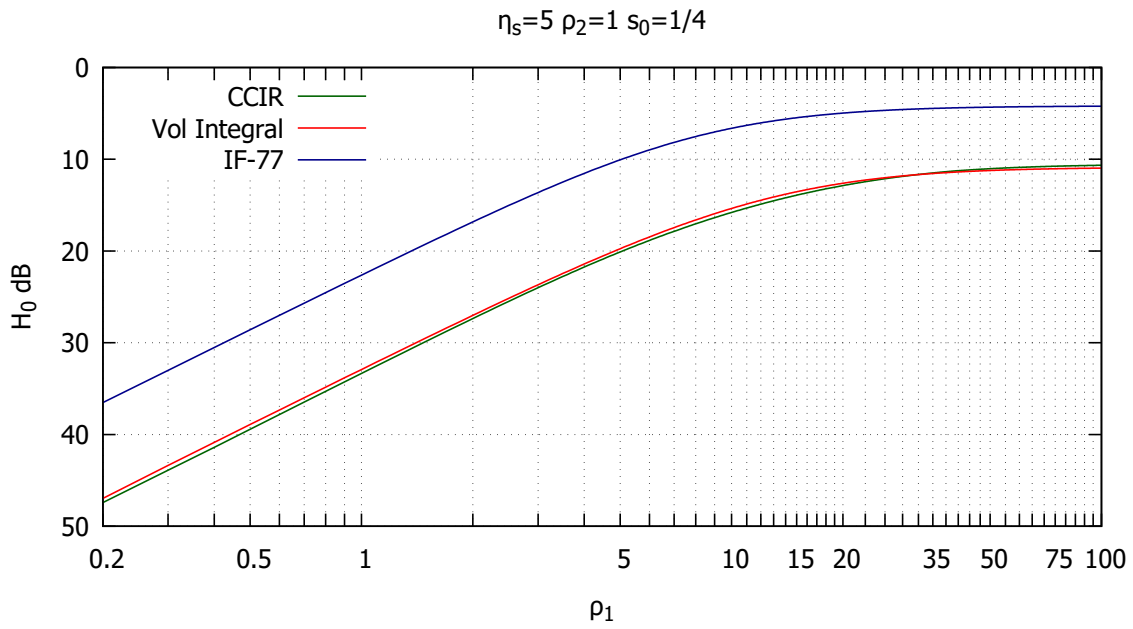


Figure 7. $\eta_s = 5$, asymmetry factor=1/4, $\rho_2 = 1$

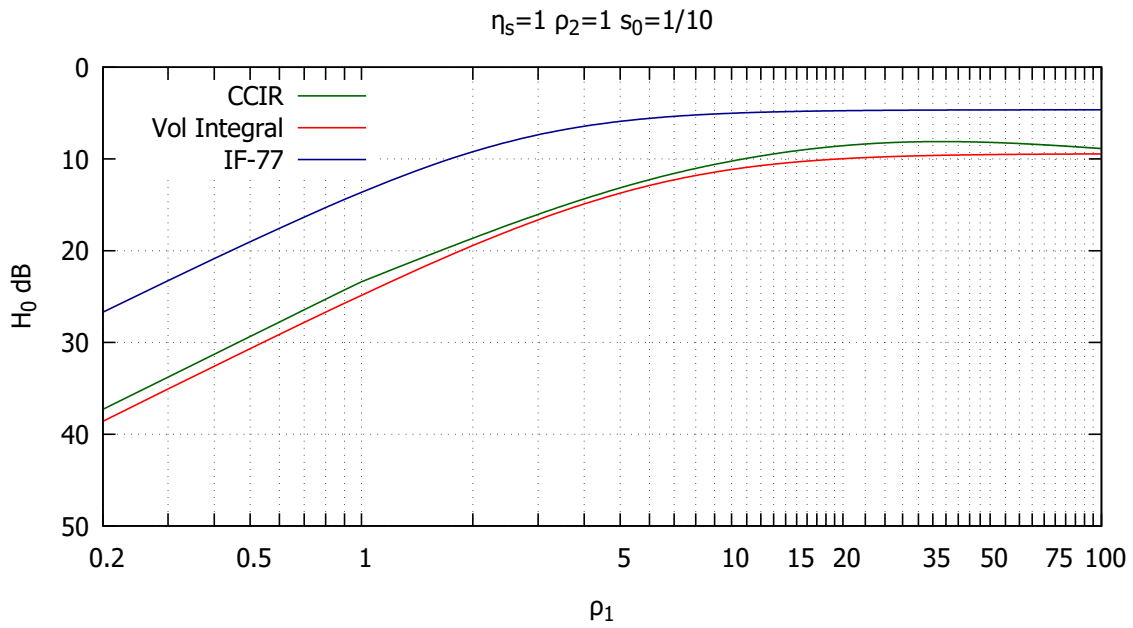


Figure 8. $\eta_s = 1$, asymmetry factor=1/10, $\rho_2 = 1$

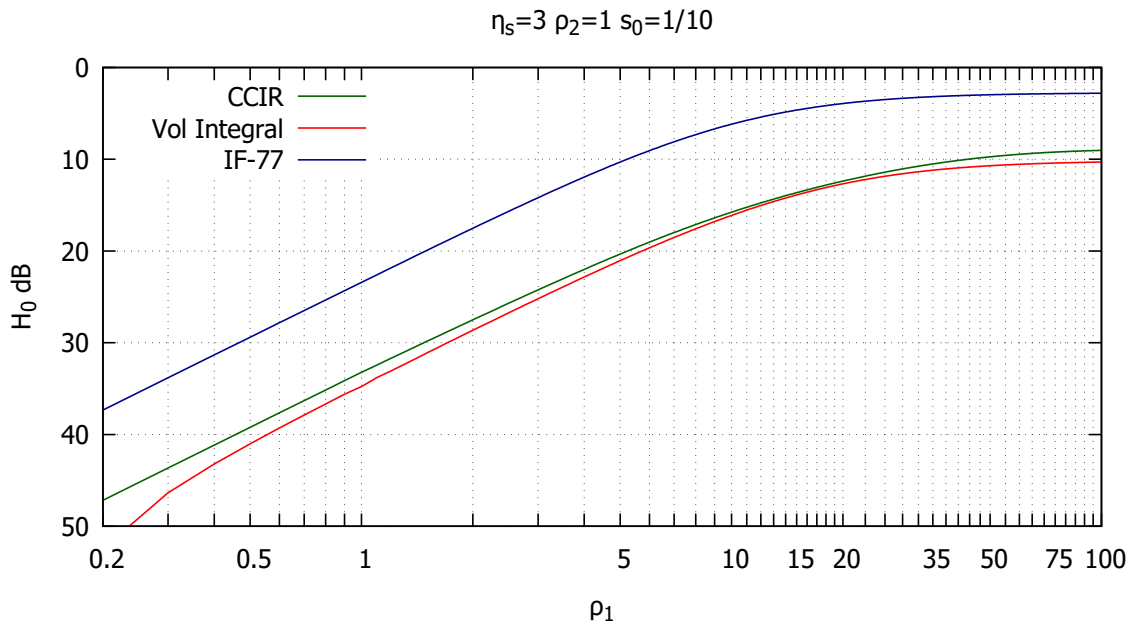


Figure 9. $\eta_s = 3$, asymmetry factor=1/10, $\rho_2 = 1$

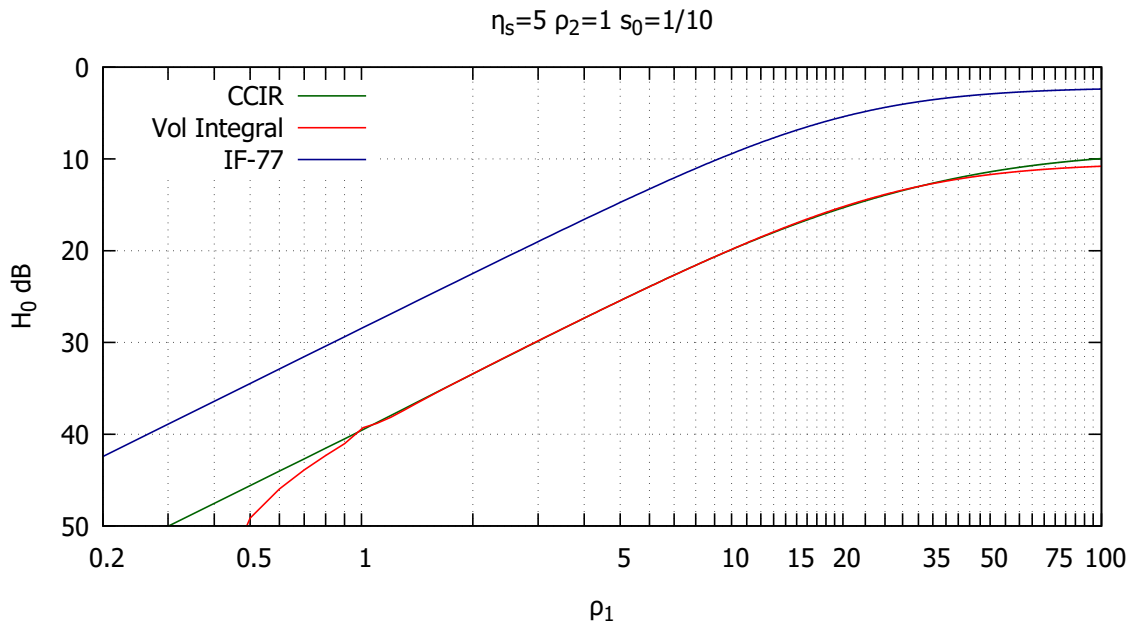


Figure 10. $\eta_s = 5$, asymmetry factor=1/10, $\rho_2 = 1$

5 CONCLUSIONS

A detailed theoretical development of a forward scatter model that culminates in the Common Volume Integral is described. This is followed by a description of methods used to evaluate the multitude of integrals that are generated. Calculations based on analytic and numerical solutions are compared with forward scatter algorithms used by ITS's propagation models (ITM, IF-73, and IF-77). Our conclusion is that the ITM and IF-73 algorithms are fairly consistent with the Common Volume Integral. IF-77 is consistent with theory if frequency gain is negligible. Otherwise there are significant differences between H_0 obtained from the IF-77 algorithm and the IF-73 algorithm. This seems odd since according to [5], the IF-73 algorithm "evolved into" the IF-77 algorithm. We do not know the reason for this difference.

6 REFERENCES

- [1] Albert D. Wheelon *Radio-wave scattering by tropospheric irregularities*, Journal of Research of the National Bureau of Standards–D. Radio Propagation, Vol. 63D No.2, September-October 1959
- [2] P. L. Rice, A. G. Longley, and K. A. Norton, *Prediction of the cumulative distribution with time of ground wave and tropospheric wave transmission loss*, NBS Technical Note 15, July 1959
- [3] P. L. Rice, A. G. Longley, K. A. Norton, and A. P. Barsis, *Transmission loss predictions for tropospheric communication circuits*, NBS Technical Note 101, Vols. 1 and 2. May 1966
- [4] George Hufford *The ITS Irregular Terrain Model, version 1.2.2, The Algorithm*
- [5] G.D. Gierhart and M.E. Johnson, *The IF-77 Electromagnetic Wave Propagation Model*, DOT/FAA/ES-83-3
- [6] J. W. herbstreit, K. A. Norton, P. L. Rice, and G. E. Schafer *Radio wave scattering in tropospheric propagation*, 1953 IRE Convention Record, Part 2, “Antennas and Communication,” pp. 85-93
- [7] K. A. Norton, et. al., *The use of angular distance in estimating transmission loss and fading range for propagation through a turbulent atmosphere over irregular terrain*, Proceedings of the IRE Vol.43, Issue 10, pp. 1488-1526, Oct. 1955
- [8] K. A. Norton, et. al., *The rate of fading in propagation through a turbulent atmosphere*, Proceedings of the IRE Vol.43, Issue 10, pp. 1341-1353, Oct. 1955
- [9] H. G. Booker and W. E. Gordon, *A theory of radio scattering in the troposphere*, Proc. IRE, vol. 38, pp. 401-412, April 1950
- [10] CCIR (1962), *Tropospheric wave transmission loss prediction*, Internatl. Radio Consultative Committee Study, Document V/23-E for question 185(V) of study program 138(V), (Internatl. Telecommunication Union, Geneva, Switzerland)
- [11] Milton Abramowitz and Irene A. Stegun, *Handbook of Mathematical Functions*, National Bureau of Standards, Applied Mathematics Series 55, June 1964
- [12] G.D. Gierhart and M.E. Johnson, *Computer programs for air/ground propagation and interference analysis 0.1 to 20 GHz*, DOT Report FAA-RD-73-103, Sept. 1973

Appendix A The Many Integrals of V^2

In this appendix, we show all of the integrals required to calculate tropospheric scatter gain. The incomplete gamma function and generalized exponential integral play an important role in what follows. Some useful relations are

$$E_n(z) = z^{n-1}\Gamma(1-n, z) = z^{n-1} \int_z^\infty \frac{e^{-t}}{t^n} dt = \frac{(-z)^{n-1}}{(n-1)!} \left[E_1(z) + e^{-z} \sum_{k=0}^{n-2} \frac{k!}{(-z)^{k+1}} \right] \quad (\text{A-1})$$

$$\Gamma(n+1, z) = n! e^{-z} \sum_{k=0}^n \frac{z^k}{k!}, \quad n \geq 0 \quad (\text{A-2})$$

$$\Gamma(0, z) = E_1(z). \quad (\text{A-3})$$

The required integrals are:

$$I_0 = \int_0^{\ell_1} \int_{\beta_0(\ell_2+x)}^\infty \frac{(\ell_1-x)^3(\ell_2+x)^3 e^{-2\gamma z}}{z^4} dz dx + \int_0^{\ell_2} \int_{\alpha_0(\ell_1+x)}^\infty \frac{(\ell_2-x)^3(\ell_1+x)^3 e^{-2\gamma z}}{z^4} dz dx, \quad (\text{A-4})$$

$$I_t = \text{Re} \left\{ e^{-i\rho_1\alpha_0} \int_0^{\ell_1} \int_{\beta_0(\ell_2+x)}^\infty \frac{(\ell_1-x)^3(\ell_2+x)^3 e^{-2\gamma z + i\rho_1 z / (\ell_1-x)}}{z^4} dz dx + e^{-i\rho_1\alpha_0} \int_0^{\ell_2} \int_{\alpha_0(\ell_1+x)}^\infty \frac{(\ell_2-x)^3(\ell_1+x)^3 e^{-2\gamma z + i\rho_1 z / (\ell_1+x)}}{z^4} dz dx \right\}, \quad (\text{A-5})$$

$$I_r = \text{Re} \left\{ e^{-i\rho_2\beta_0} \int_0^{\ell_1} \int_{\beta_0(\ell_2+x)}^\infty \frac{(\ell_1-x)^3(\ell_2+x)^3 e^{-2\gamma z + i\rho_2 z / (\ell_2+x)}}{z^4} dz dx + e^{-i\rho_2\beta_0} \int_0^{\ell_2} \int_{\alpha_0(\ell_1+x)}^\infty \frac{(\ell_2-x)^3(\ell_1+x)^3 e^{-2\gamma z + i\rho_2 z / (\ell_2-x)}}{z^4} dz dx \right\}, \text{ and} \quad (\text{A-6})$$

$$I_{t\pm r} = \text{Re} \left\{ e^{-i(\rho_1\alpha_0 \pm \rho_2\beta_0)} \int_0^{\ell_1} \int_{\beta_0(\ell_2+x)}^\infty \frac{(\ell_1-x)^3(\ell_2+x)^3 e^{-2\gamma z + iz[\rho_1/(\ell_1-x) \pm \rho_2/(\ell_2+x)]}}{z^4} dz dx + e^{-i(\rho_1\alpha_0 \pm \rho_2\beta_0)} \int_0^{\ell_2} \int_{\alpha_0(\ell_1+x)}^\infty \frac{(\ell_2-x)^3(\ell_1+x)^3 e^{-2\gamma z + iz[\rho_1/(\ell_1+x) \pm \rho_2/(\ell_2-x)]}}{z^4} dz dx \right\}; \quad (\text{A-7})$$

the tropospheric scatter gain is then

$$V^2 = \underbrace{\left[\frac{4}{3\pi^2} S_0 \right]}_{10^{-S_e/10}} e^{2\gamma h_0} \left(\frac{\ell}{\theta^3 k} \right) \frac{\theta^3}{\ell^4} [I_0 - I_t - I_r + (I_{t+r} + I_{t-r})/2] \quad (\text{A-8})$$

where S_e is the scattering efficiency term found in [5].

We can make this a bit more compact by changing variables and writing the integral over z in terms of the generalized exponential integral $E_4(z)$:

$$I_0 = \frac{1}{\beta_0^3} \int_{\ell_2}^{\ell} (\ell - w)^3 E_4(2\gamma\beta_0 w) dw + \frac{1}{\alpha_0^3} \int_{\ell_1}^{\ell} (\ell - w)^3 E_4(2\gamma\alpha_0 w) dw, \quad (\text{A-9})$$

$$I_t = \text{Re} \left\{ e^{-i\rho_1\alpha_0} \left[\frac{1}{\beta_0^3} \int_{\ell_2}^{\ell} (\ell - w)^3 E_4 \left(\beta_0 w \left[2\gamma - \frac{i\rho_1}{\ell - w} \right] \right) dw + \frac{1}{\alpha_0^3} \int_{\ell_1}^{\ell} (\ell - w)^3 E_4 \left(\alpha_0 w \left[2\gamma - \frac{i\rho_1}{w} \right] \right) dw \right] \right\}, \quad (\text{A-10})$$

$$I_r = \text{Re} \left\{ e^{-i\rho_2\beta_0} \left[\frac{1}{\beta_0^3} \int_{\ell_2}^{\ell} (\ell - w)^3 E_4 \left(\beta_0 w \left[2\gamma - \frac{i\rho_2}{w} \right] \right) dw + \frac{1}{\alpha_0^3} \int_{\ell_1}^{\ell} (\ell - w)^3 E_4 \left(\alpha_0 w \left[2\gamma - \frac{i\rho_2}{\ell - w} \right] \right) dw \right] \right\}, \text{ and} \quad (\text{A-11})$$

$$I_{t\pm r} = \text{Re} \left\{ e^{-i(\rho_1\alpha_0 \pm \rho_2\beta_0)} \left[\frac{1}{\beta_0^3} \int_{\ell_2}^{\ell} (\ell - w)^3 E_4 \left(\beta_0 w \left[2\gamma - i \left(\frac{\rho_1}{\ell - w} \pm \frac{\rho_2}{w} \right) \right] \right) dw + \frac{1}{\alpha_0^3} \int_{\ell_1}^{\ell} (\ell - w)^3 E_4 \left(\alpha_0 w \left[2\gamma - i \left(\frac{\rho_1}{w} \pm \frac{\rho_2}{\ell - w} \right) \right] \right) dw \right] \right\}. \quad (\text{A-12})$$

Modulus of Asymmetry

Following [5] we will describe the integrals in terms of the modulus of asymmetry $s = (\ell_1 - \ell_2)/\ell$. Evidently this mechanism allows us to replace α_0 and β_0 with θ and $\ell_{1,2}$ with ℓ using the following relations:

$$\ell_1 = \ell(1+s)/2, \quad \ell_2 = \ell(1-s)/2, \quad \alpha_0 = \theta(1-s)/2, \quad \beta_0 = \theta(1+s)/2.$$

We then have

$$I_0 = \frac{8}{\theta^3} \left[\frac{1}{(1+s)^3} \int_{\ell(1-s)/2}^{\ell} (\ell-w)^3 \mathbf{E}_4 \left(2\gamma\theta w \frac{1+s}{2} \right) dw + \frac{1}{(1-s)^3} \int_{\ell(1+s)/2}^{\ell} (\ell-w)^3 \mathbf{E}_4 \left(2\gamma\theta w \frac{1-s}{2} \right) dw, \right] \quad (\text{A-13})$$

$$I_t = \frac{8}{\theta^3} \operatorname{Re} \left\{ e^{-i\rho_1 \frac{1-s}{2}} \left[\frac{1}{(1+s)^3} \int_{\ell(1-s)/2}^{\ell} (\ell-w)^3 \mathbf{E}_4 \left(\frac{\theta w(1+s)}{2} \left[2\gamma - \frac{i\rho_1}{\ell-w} \right] \right) dw + \frac{1}{(1-s)^3} \int_{\ell(1+s)/2}^{\ell} (\ell-w)^3 \mathbf{E}_4 \left(\frac{\theta w(1-s)}{2} \left[2\gamma - \frac{i\rho_1}{w} \right] \right) dw \right] \right\}, \quad (\text{A-14})$$

$$I_r = \frac{8}{\theta^3} \operatorname{Re} \left\{ e^{-i\rho_2 \frac{1+s}{2}} \left[\frac{1}{(1+s)^3} \int_{\ell(1-s)/2}^{\ell} (\ell-w)^3 \mathbf{E}_4 \left(\frac{\theta w(1+s)}{2} \left[2\gamma - \frac{i\rho_2}{w} \right] \right) dw + \frac{1}{(1-s)^3} \int_{\ell(1+s)/2}^{\ell} (\ell-w)^3 \mathbf{E}_4 \left(\frac{\theta w(1-s)}{2} \left[2\gamma - \frac{i\rho_2}{\ell-w} \right] \right) dw \right] \right\}, \text{ and} \quad (\text{A-15})$$

$$I_{t\pm r} = \frac{8}{\theta^3} \operatorname{Re} \left\{ e^{-i(\rho_1 \frac{1-s}{2} \pm \rho_2 \frac{1+s}{2})} \left[\frac{1}{(1+s)^3} \int_{\ell(1-s)/2}^{\ell} (\ell-w)^3 \mathbf{E}_4 \left(\frac{\theta w(1+s)}{2} \left[2\gamma - i \left(\frac{\rho_1}{\ell-w} \pm \frac{\rho_2}{w} \right) \right] \right) dw + \frac{1}{(1-s)^3} \int_{\ell(1+s)/2}^{\ell} (\ell-w)^3 \mathbf{E}_4 \left(\frac{\theta w(1-s)}{2} \left[2\gamma - i \left(\frac{\rho_1}{w} \pm \frac{\rho_2}{\ell-w} \right) \right] \right) dw \right] \right\}. \quad (\text{A-16})$$

Appendix B Constant Refractivity Frequency Gain

For this case we set $\eta = 0$, $s = 0$, $A = 0$, and $f(w) = B + C/(\ell - w)$. Referring to Appendix A, the required integrals are

$$J(B, C, \mu) = \int_{\mu\ell}^{\ell} (\ell - w)^3 f^3(w) \Gamma(-3, f(w)) dw \quad (\text{A-17})$$

$$K(\rho, \mu) = E_4\left(\frac{-i\rho}{2}\right) \int_{\mu\ell}^{\ell} (\ell - w)^3 dw = \frac{\ell^4(1-\mu)^4}{4} E_4\left(\frac{-i\rho}{2}\right). \quad (\text{A-18})$$

Noting that

$$\frac{d}{dw} \Gamma(-3, f(w)) = -\frac{f'(w)e^{-f(w)}}{[f(w)]^4} \quad (\text{A-19})$$

$$\int (\ell - w)^3 f^3(w) dw = -\frac{[(\ell - w)f(w)]^4}{4B} \quad (\text{A-20})$$

partial integration yields

$$J(B, C, \mu) = -\left[\frac{[(\ell - w)f(w)]^4}{4B} \Gamma(-3, f(w)) + \frac{Ce^{-B}}{4B} \int (\ell - w)^2 e^{-C/(\ell - w)} dw \right]_{\mu\ell}^{\ell} \quad (\text{A-21})$$

$$= -\frac{(\ell - w)^3}{4B} \left[(B(\ell - w) + C) E_4\left(B + \frac{C}{\ell - w}\right) - Ce^{-B} E_4\left(\frac{C}{\ell - w}\right) \right]_{\mu\ell}^{\ell} \quad (\text{A-22})$$

$$= \frac{\ell^4(1-\mu)^3}{4B} \left[(B(1-\mu) + C/\ell) E_4\left(B + \frac{C/\ell}{1-\mu}\right) - C/\ell e^{-B} E_4\left(\frac{C/\ell}{1-\mu}\right) \right]. \quad (\text{A-23})$$

For constant refractivity we set $\mu^{(1)} = \mu^{(2)} = \mu = 1/2$,

$$B_t^{(1)} = \frac{i\rho_1}{2}, \quad B_t^{(2)} = n/a, \quad B_r^{(1)} = n/a, \quad B_r^{(2)} = \frac{i\rho_2}{2},$$

$$B_{t+r}^{(1)} = \frac{i(\rho_1 - \rho_2)}{2}, \quad B_{t+r}^{(2)} = \frac{i(\rho_2 - \rho_1)}{2},$$

$$B_{t-r}^{(1)} = \frac{i(\rho_1 + \rho_2)}{2}, \quad B_{t-r}^{(2)} = -\frac{i(\rho_1 + \rho_2)}{2},$$

$$C^{(1)} = -\frac{i\rho_1\ell}{2}, \quad C^{(2)} = -C^{*(2)} = -\frac{i\rho_2\ell}{2}$$

yielding

$$I_t = \frac{8}{\theta^3} \operatorname{Re} \left\{ e^{\frac{-i\rho_1}{2}} \left[J(B_t^{(1)}, C^{(1)}, \mu) + K(\rho_2, \mu) \right] \right\} \quad (\text{A-24})$$

$$I_r = \frac{8}{\theta^3} \operatorname{Re} \left\{ e^{\frac{-i\rho_2}{2}} \left[K(\rho_1, \mu) + J(B_r^{(2)}, C^{(2)}, \mu) \right] \right\} \quad (\text{A-25})$$

$$I_{t+r} = \frac{8}{\theta^3} \operatorname{Re} \left\{ e^{-i\left(\frac{\rho_1+\rho_2}{2}\right)} \left[J(B_{t+r}^{(1)}, C^{(1)}, \mu) + J(B_{t+r}^{(2)}, C^{(2)}, \mu) \right] \right\} \quad (\text{A-26})$$

$$I_{t-r} = \frac{8}{\theta^3} \operatorname{Re} \left\{ e^{-i\left(\frac{\rho_1-\rho_2}{2}\right)} \left[J(B_{t-r}^{(1)}, C^{(1)}, \mu) + J(B_{t-r}^{(2)}, C^{*(2)}, \mu) \right] \right\}. \quad (\text{A-27})$$

After some tedious arithmetic we find

$$I_t = \frac{\ell^4}{4\theta^3} \operatorname{Re} \left\{ e^{-i\rho_1} E_4(-i\rho_1) \right\} \quad (\text{A-28})$$

$$I_r = \frac{\ell^4}{4\theta^3} \operatorname{Re} \left\{ e^{-i\rho_2} E_4(-i\rho_2) \right\} \quad (\text{A-29})$$

$$I_{t+r} = \frac{\ell^4}{4\theta^3(\rho_1 - \rho_2)} \operatorname{Re} \left\{ \rho_1 e^{-i\rho_1} E_4(-i\rho_1) - \rho_2 e^{-i\rho_2} E_4(-i\rho_2) \right\} \quad (\text{A-30})$$

$$I_{t-r} = \frac{\ell^4}{4\theta^3(\rho_1 + \rho_2)} \operatorname{Re} \left\{ \rho_1 e^{-i\rho_1} E_4(-i\rho_1) + i\rho_2 e^{i\rho_2} E_4(i\rho_2) \right\}. \quad (\text{A-31})$$

and

$$\frac{1}{2}(I_{t+r} + I_{t-r}) = \frac{\ell^4}{4\theta^3(1 - \rho_2^2/\rho_1^2)} \operatorname{Re} \left\{ e^{-i\rho_1} E_4(-i\rho_1) - \frac{\rho_2^2}{\rho_1^2} e^{-i\rho_2} E_4(-i\rho_2) \right\}. \quad (\text{A-32})$$

The frequency gain function is

$$H_0 = -10 \log \left[1 - \frac{I_t - I_r + (I_{t+r} + I_{t-r})/2}{I_0} \right]. \quad (\text{A-33})$$

Previously we found that $I_0 = \ell^4/(12\theta^3)$ and then

$$H_0 = -10 \log \left[\operatorname{Re} \left\{ 1 + \frac{3}{1 - \rho_2^2/\rho_1^2} \left(\frac{\rho_2^2}{\rho_1^2} e^{-i\rho_1} E_4(-i\rho_1) - e^{-i\rho_2} E_4(-i\rho_2) \right) \right\} \right]. \quad (\text{A-34})$$

BIBLIOGRAPHIC DATA SHEET

1. Publication Number TR-22-557		2. Government Accession Number	3. Recipient's Accession Number
4. Title and Subtitle Tropospheric Scatter: Theory vs. Predictive Models		5. Publication Date February 28, 2022	
		6. Performing Organization Code	
7. Author(s) Roger Dalke		9. Project/Task/Work Unit No. 3111012-300	
8. Performing Organization Name and Address Institute for Telecommunication Sciences, National Telecommunications & Information Administration, U.S. Department of Commerce 325 Broadway Boulder, CO 80305		10. Contract/Grant Number	
		12. Type of Report and Period Covered	
11. Sponsoring Organization Name and Address Institute for Telecommunication Sciences, National Telecommunications & Information Administration U.S. Department of Commerce 325 Broadway Boulder, CO 80305			
14. Supplementary Notes			
15. ABSTRACT <i>(A 200-word or less factual summary of most significant information. If document includes a significant bibliography or literature survey, mention it here.)</i> Circa 1960, the National Bureau of Standards intensively studied over-the-horizon radio propagation due to tropospheric (aka forward) scatter. The results of that effort, published in the form of graphs and/or empirical mathematical functions based on curve fitting, led to the development of important radio propagation models. Unfortunately, there is scant documentation describing exactly how the published data is related to the underlying theoretical basis for scattering theory. In this report, we describe the electromagnetic theory that results in the forward scatter Common Volume Integral. This is followed by a description of analytical methods used to obtain solutions. The results are then compared to propagation model predictions. In general, fairly good agreement between theory and models was obtained for the Irregular Terrain Model and IF-73 air/ground propagation model. Good agreement with the IF-77 Electromagnetic Wave Propagation Model was obtained when frequency gain corrections are negligible. Otherwise, the IF-77 and theoretical results differed significantly. The reason for this was not determined.			
16. Key Words <i>(Alphabetical order, separated by semicolons)</i> tropospheric scatter, forward scatter, Irregular Terrain Model, IF-77 Electromagnetic Wave Propagation Model			
17. Availability Statement <input checked="" type="checkbox"/> Unlimited <input type="checkbox"/> For Official Distribution		18. Security Class. (This report) Unclassified	20. Number of Pages 38
		19. Security Class. (This page) Unclassified	21. Price N/A

NTIA FORMAL PUBLICATION SERIES

NTIA MONOGRAPH (MG)

A scholarly, professionally oriented publication dealing with state-of-the-art research or an authoritative treatment of a broad area. Expected to have long-lasting value.

NTIA SPECIAL PUBLICATION (SP)

Conference proceedings, bibliographies, selected speeches, course and instructional materials, directories, and major studies mandated by Congress.

NTIA REPORT (TR)

Important contributions to existing knowledge of less breadth than a monograph, such as results of completed projects and major activities.

JOINT NTIA/OTHER-AGENCY REPORT (JR)

Important contributions to existing knowledge of less breadth than a monograph, such as results of completed projects and major activities.

NTIA SOFTWARE & DATA PRODUCTS (SD)

Software such as programs, test data, and sound/video files. This series can be used to transfer technology to U.S. industry.

NTIA HANDBOOK (HB)

Information pertaining to technical procedures, reference and data guides, and formal user's manuals that are expected to be pertinent for a long time.

NTIA TECHNICAL MEMORANDUM (TM)

Technical information typically of less breadth than an NTIA Report. The series includes data, preliminary project results, and information for a specific, limited audience.

For information about NTIA publications, contact the NTIA/ITS Technical Publications Office at 325 Broadway, Boulder, CO, 80305 Tel. (303) 497-3572 or e-mail ITSinfo@ntia.gov.